Contents lists available at ScienceDirect

Atmospheric Research

journal homepage: http://ees.elsevier.com

Analysis of sounding derived parameters and application to severe weather events in the Canary Islands

David Suárez Molina [a], Sergio Fernández-González [a,*], Juan Carlos Suárez González [a], Albert Oliver [b]

[a] State Meteorological Agency (AEMET), Spain
[b] University Institute for Intelligent Systems and Numerical Applications in Engineering (SIANI), University of Las Palmas de Gran Canaria, Spain

ARTICLE INFO

Keywords
Soundings
Deep convection
Subtropical atmosphere
Severe weather events

ABSTRACT

Severe weather phenomena have serious consequences in Canary Islands. This archipelago is located in the subtropical Atlantic Ocean, west of North Africa. For this reason, its climatic characteristics differ greatly from those of mainland Spain. The importance of forecasting convective precipitation mainly lies in the damage caused by flooding. Therefore, an adequate knowledge of the thresholds for the convective indices associated with severe thunderstorms in the Canary Islands is crucial for minimizing the damage that these events cause.In this paper, 7021 soundings from the Güimar station (id = 60,018, Tenerife, Spain) during the period 2009–2018 were analysed. Observation data are used to categorize soundings as representative of conditions for no thunder episodes, general thunder, rainfall ≥15 mm/h, rainfall ≥30 mm/h and hail or wind gusts ≥120 km/h. From sounding data, several parameters were computed. For some parameters, the results show remarkable differences between categories. In the studied region, thunderstorms are not expected when CAPE values are close to 0 J/kg and the lapse rate in the 0–3 km layer is below 5 °C/km. On the other hand, heavy rainfall events (rainfall ≥30 mm/h) show the highest median of CAPE, a high median total precipitable water (TPW, close to 30 mm) and the lapse rate decreases with height. Finally, hailstorm events are characterized by High Shear (shear vector magnitude ≥35 kt) and Low CAPE (surface-based CAPE ≤500 J/kg and most unstable parcel CAPE ≤1000 J/kg) environments (HSLC).

1. Introduction

Deep convection is related to the transfer of moisture and latent heat by updrafts and downdrafts, causing meteorological risks such as strong wind gusts, heavy rain, and sometimes lightning and hail (García-Ortega et al., 2014). As a result, severe thunderstorms cause dramatic damage to properties and even fatalities every year in many regions around the world (Czernecki et al., 2016). In addition, air traffic management is strongly affected by adverse weather conditions caused by deep convection (Borsky and Unterberger, 2019). As far as aviation safety is concerned, deep convection results in problems related to turbulence, wind shear, aircraft icing, and low visibility events (Bolgiani et al., 2018). The Canary Islands are not exempt from this risk, with several cases of flash floods recorded in recent decades (Génova et al., 2015).

The analysis of the pre-convective atmospheric environment is vital when estimating the risk of severe thunderstorms events (Brooks et al., 2003). In this regard, the use of radiosonde data has proven to be useful (Sánchez et al., 2007). Thereby, the comparison between pre-convective radio soundings during severe and non-severe thunderstorm events permits the categorization of the atmospheric conditions related to deep convection (Púcik et al., 2015). In the same way, Taszarek et al. (2017) analyse the thermodynamic and kinematic variables capable of differentiating among the atmospheric conditions prone to severe and non-severe thunderstorms, distinguishing between gale-force wind gusts, large hail, and even tornadoes.

Convective storms are commonly connected with weather patterns on the synoptic scale. However, the worst effects of these events usually affect a lesser area, hindering forecasting. There are at least three essential requirements for the development of severe thunderstorms: a deep unstable layer, high moisture content in the boundary layer, and a trigger mechanism responsible for the activation of the convection process (Gascón et al., 2015). In southwestern Europe, thermal instability and low-level convergence associated with dynamic instability are the main triggers of convection (Merino et al., 2019).

The adverse effects of severe thunderstorms over human activities can be diminished by having a better knowledge of this kind of meteorological phenomenon, allowing the development of early warning systems and forecasting models to minimize economic losses and even saving human lives (Bauer et al., 2015; García-Ortega et al., 2017

* Corresponding author at: Delegación Territorial de AEMET en Cantabria, C/Ricardo Lorenzo, s/n 39012 Cueto - Santander, Cantabria, Spain.
E-mail address: sfernandezg@aemet.es (S. Fernández-González)

https://doi.org/10.1016/j.atmosres.2020.104865
Received 11 September 2019; Received in revised form 30 December 2019; Accepted 15 January 2020
Available online xxx
0169-8095/

). Due to the low performance of traditional forecasting methods in the forecast of deep convection, subjective methods based on stability indices and thermodynamic conditions were developed in order to identify the most favourable conditions for the occurrence of thunderstorms (López et al., 2007). However, no single index works best in all locations, or for all types of severe weather, such as wind, large hail, heavy precipitation or tornadoes (Doswell III, 1987). As a result, the indices calculated for a specific area cannot be extrapolated to other regions. In fact, the values of stability indices in Europe tend to be lower than in North America or tropical latitudes (López et al., 2001). It is known that the performance of convection indices is highly dependent upon the features of the specific area of the world (Charba, 1979), which suggests the need to estimate the thresholds of the indices associated with a certain severity of convective episodes in a specific region.

Stability indices can be calculated by analysing radiosonde data. Radiosondes have a high vertical resolution, capable of defining the bases and thicknesses of cloud layers and stable layers. They also give the only operationally available upper-air data with an absolute calibration (Lorenc et al., 1996). This is the methodology chosen in this research, in which ten years of radiosonde profiles were analysed, categorizing the events within 5 categories depending on the observational data. Subsequently, the thresholds of several stability indices related to different categories of convective episodes are estimated, with the aim of providing this information to bench forecasters during the decision-making process, helping them in the evaluation of risks associated to severe convection.

The paper is organized as follows. A brief description of the study area is covered in Section 2. Section 3 summarizes the database used in this research. Subsequently, Section 4 presents the main results of this research and the discussion, including an analysis of several convection indexes and an examination of case studies. Finally, the main conclusions of this paper are provided in Section 5.

2. Study area

The Canary archipelago (Fig. 1), which is located west of North Africa, consists of seven islands with a total area of about 7200 km^2, 1100 km from mainland Spain. Covering from 27°37′ to 29°25′N and from 18°10′ to 13°20′W, all islands belong to the subtropical zone. Canary Islands are under the direct influence of the trade wind belt, making the climate very stable all year. Usually, the Azores high acts as a shield, preventing Atlantic lows from affecting the area south of 30°N. Moreover the islands are surrounded by the Canary Current, coming from the north as a cold derivation of the Gulf Stream (Herrera et al., 2001). The average trade winds blow mainly against the north side of the islands, advecting wet and fresh air, which can rise over the island slopes, often leading to condensation and cloud growth that is usually obstructed by the typical vertical stratification structure (Font, 1956). Therefore, three main layers can be distinguished:

1) Relatively fresh and moist air exists at low levels, due to the cold surface water of the Canaries Current.
2) A subsidence inversion is usually found roughly between 700 and 1500 masl (meters above sea level). Temperature increases across this layer up to 6 °C, acting as a lid that obstructs any convective development, even those forced by the orography.
3) Over the inversion layer, the air is dry and clear.

In this way, water vapour is condensed at low levels, under the inversion layer, developing non precipitating thin clouds, which are called "cloud sea" when viewed from above the clouds' top. As a result, the typical weather on Canary Islands is very stable and dry. Rainy events only happen when disturbances break the inversion layer, either at surface (Atlantic lows) or at upper levels (troughs). The importance of high-level disturbances on the islands' precipitation must be emphasized. Most of the typical rainfall situations cannot be detected at surface level, and are only evident when upper levels are analysed.

2.1. Weather impact on the Canary Islands

In spite of the apparent climatic mildness, the frequency and intensity of the severe weather events have serious consequences on the Canary Islands (Dorta, 2007). To contextualize the impact that severe weather events have in the Canary Islands, statistics on fatalities due to natural hazards in the Canary Islands can be used. In the period from 1995 to 2014 there have been a total of 74 fatalities due to disasters caused by severe weather events. According to information provided by the CCS (Consorcio de Compensación de Seguros, a public organization funded by the Ministry of Economy, Industry and Competitiveness), the losses in economic terms due to floods and windstorms in the Canary Islands throughout the period 1996–2018, amounted to >211 million Euros.

One of the biggest impacts is caused by flooding and landslides due to intense rainfall. Precipitation is very rare and localized, which makes them more destructive since neither the infrastructures nor the popula-

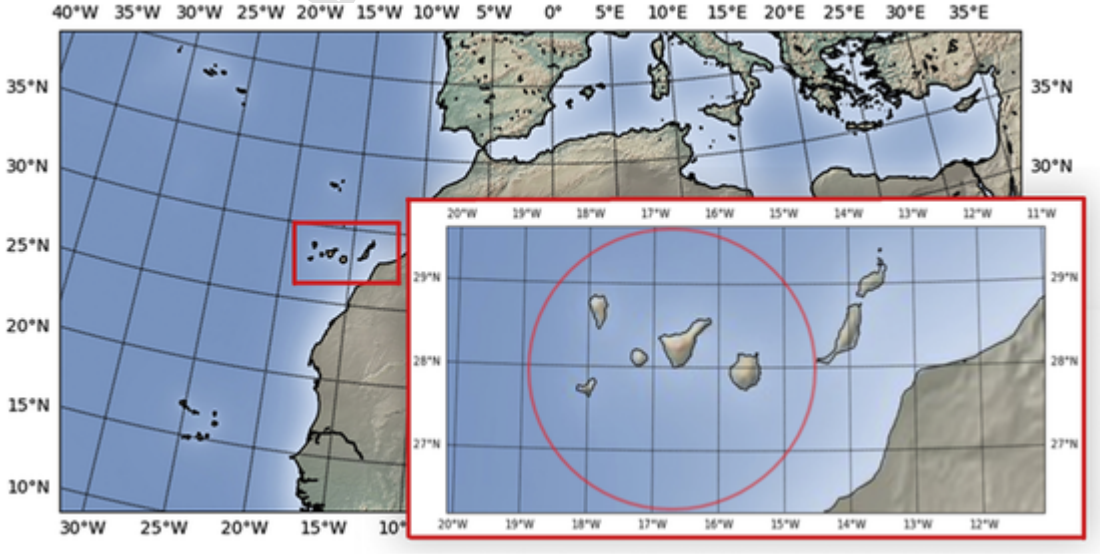

Fig. 1. Study area, with a zoom of Canary Islands. The red circle indicates the 200 km threshold of the radio sounding representativeness. The red dot highlights station number 60018 (Güimar, Tenerife). (For interpretation of the references to colour in this figure legend, the reader is referred to the web version of this article.)

tion are prepared to face them. The spatial and temporal concentration of rainfall in Canary Islands is therefore a severe hazard, which together with the high vulnerability creates extreme risk situations (Suárez-Molina et al., 2018). The origin of situations of extreme adversity must be sought in the action of high level troughs and cut-off lows, with marked thermal instability that leads to deep convection associated with some processes by which an air parcel is lifted to its level of free convection (LFC).The lift required to raise an air parcel to its LFC generally must be supplied by some processes operating at subsynoptic-scale, because the rising motions associated with synoptic-scale processes usually are too slow to lift a potentially buoyant parcel to its LFC in the required time (Doswell III, 1987). Tropical factors may have an essential role during some events, such as a disturbance of tropical origin, or indirectly, the interaction of the polar front with maritime tropical air masses of high moisture content.

3. Methods

3.1. Proximity criteria

Radio sounding data at 00 and 12 UTC from the station number 60018 located in Güimar (Tenerife) were collected for the period 2009–2018. A proximity criteria of 200 km from the sounding release location (represented by a red circle in Fig. 1) was defined, with a temporal representativeness covering the period from 09 to 15 UTC and 21–03 UTC (6 h period centred on the 00 and 12 UTC soundings). The 200 km threshold lies within the range of the 80-km used by Darkow (1969), Schaefer and Livingston (1988) and Brooks et al. (1994) and 400-km criteria utilized by Rasmussen and Blanchard (1998). The 200 km threshold was also selected because of the different behaviour of rainfall in the easternmost islands (Lanzarote and Fuerteventura) in relation to the rest of the archipelago. According to Herrera et al. (2001), annual precipitation behaviour of the five western islands is very similar, while Lanzarote and Fuerteventura form an appreciably separated cluster (Herrera et al., 2001). As a result, Güimar radiosonde is not representative of the atmospheric conditions on Lanzarote and Fuerteventura due to the proximity to the African continent and the influence of the Saharan Air Layer.

3.2. Criteria for event selection

Observational data for the period from January 1, 2009 to December 31, 2018 were used. These data were extracted from the AEMET observational database and have been used to divide the dataset into 5 categories (Table 1). The categories are exclusive, and each event was assigned using the most severe observation (i.e., a wind gust ≥120 km/h or hail event was assigned only in category 5, even if rainfall ≥30 mm /h also occurred). Therefore, an event is only included in one category, although in that event it meets several criteria. The classification criteria is exclusive and it is in descending order (category 5, category 4, category 3 and so on).

The lightning strike threshold of two or more cloud-to-ground (CG) strikes is consistent with the criteria established by Reap (1986) and R. Orville (2001, personal communication), similar to the >3-CG strike threshold used by Hamill and Church (2000), but much less than the >10-CG strike criteria used by Rasmussen and Blanchard (1998).

Table 1
Definitions and number of proximity soundings for the five categories.

Category	Definition	Quantity
1	No thunder or < 2 CG strikes	6791
2	General thunder (≥ 2 CG strikes)	58
3	Rainfall ≥15 mm/h	81
4	Rainfall ≥30 mm/h	34
5	Hail or wind gust ≥120 km/h at least in 2 locations	57

Categories 3 and 4 agree with the 1 h rainfall thresholds established in the National Plan of Prediction and Surveillance of Adverse Meteorological Phenomena (METEOALERTA, 2018), elaborated by AEMET in coordination with Spanish Civil Protection Authorities, for the interest area. At least 2 observations are necessary in category 5 in order to avoid singular points. This is because in high areas of Tenerife (e.g., Izaña is located at 2371 m above sea level) many days wind gusts ≥ 120 km/h of non-convective origin are recorded. To illustrate this local effect, the automatic meteorological station network of the Canary Islands was used. The wind gust threshold of 120 km/h was exceeded in Izaña in 54 days. In contrast, the location with the second most threshold exceedances was La Palma airport with only 8 days.

No attempt was made to modify the soundings. It was anticipated that the effects of unrepresentative, contaminated, or erroneous data would be damped out in the statistical analysis (Craven and Brooks, 2004).

3.3. Sounding derived parameters

A list of the parameters computed from the sounding dataset is shown in Table 2. One often underappreciated aspect of computing CAPE is the effect of moisture on the calculation. For this reason all CAPE values were calculated using the virtual temperature correction (Doswell III and Rasmussen, 1994). Different air parcels are being used to calculate CAPE. The prefixes MU, ML and SB have been designed to identify air parcels. MU is the most unstable parcel found in the lowest 300 hPa of the atmosphere, ML represents the mean conditions in the lowest 100 hPa, while SB is the surface based parcel. The SB parcel choice uses the surface air and dew point temperatures to determine the parcel ascent path.

Although it allows a better representation of surface-based convection, calculations can be highly dependent on small time and space scales when these thermodynamic parameters display significant variations. The ML parcel choice is used to lift a parcel constituting a well-mixed layer of constant potential temperature and mixing ratio. Due to the averaging properties of the ML parcel choice, it is less variable in time and space than SB. Values of ML are typically smaller than those of SB. The ML and SB will be equal when the boundary layer is well mixed throughout the lifting layer. The MU will always produce the largest estimation of buoyancy among the three measures introduced above. There is an ongoing discussion as to what the best choice is. It seems that every forecaster has his own preference. Due to the high sensitivity of CAPE for minor changes in temperature and dew point one should always be aware of which CAPE one is considering. In order to characterize and to establish CAPE thresholds to the different categories defined in Table 1 for the area of interest, ML, MU and SB parcels were used.

Table 2
Parameters computed from soundings (m AGL refers to meters above ground level).

Parameter	Units
MUCAPE	J/kg
MLCAPE	J/kg
SBCAPE	J/kg
0–3 km Lapse Rate	°C/km
3–6 km Lapse Rate	°C/km
700–500 hPa Lapse Rate	°C/km
850–700 hPa Lapse Rate	°C/km
LCL height (lifted condensation level)	m AGL
0–1 km Bulk shear	kt
0–3 km Bulk shear	kt
0–6 km Bulk shear	kt
Total precipitable water	mm

4. Results and Discussion

4.1. Analysis of convection indexes

In this section, box-and-whisker plots (Tukey, 1977) are used extensively to compare data in each category. Boxplot essentially presents a quick sketch of the distribution of the underlying data. Boxplots can convey a surprisingly large amount of information at a glance. Median and quartiles of the boxplot are highly robust and resistant to any outliers that might be present. One important use of box plots is the simultaneous graphical comparison of several batches of data (Wilks, 2011).

4.1.1. CAPE

During the forecasting of deep convection episodes, one of the main problems an operational forecaster faces is determining a representative value of potential instability. Deciding which parcel to "lift" in the computation of CAPE is crucial in this diagnostic process (Craven et al., 2002). The choice of different parcels for the computation of CAPE (Fig. 2) shows an overlap between categories. However, it is possible to discriminate in most cases category 1 from the rest since the values are close to 0 J/kg. There is overlap between category 1 and 5 for the MLCAPE. However, this category presents higher distribution values of MUCAPE (median = 21 J/kg) and SBCAPE (median = 17 J/kg) than category 1. Typical soundings of category 5 are called "inverted-V" since the dew point depression decreases significantly with height. These events have dry air in the lower troposphere with nearly saturated air in the middle troposphere. As will be seen later, convection tends to be high based since the Convective Condensation Level is at a high elevation. Due to negative buoyancy related to latent cooling of evaporation aloft that causes it to accelerate toward the surface, strong winds are the most common severe weather[1]. Hail or wind gusts higher than 120 km/h events (category 5) are characterized by low CAPE environments.

Situations categorized as type 2, 3 and 4 show the largest median differences between SBCAPE and MUCAPE. However, categories 2 and 3 have SBCAPE medians close to 0 J/kg and category 4 has a SBCAPE median of 485 J/kg. In the categories 2 and 3 low values of SBCAPE can be explained because convective storms may be sustained by air feeding the updraft from this level. It is likely to occur, when the surface layer may be substantially cooler than the air above it. In that case, it is more appropriate to calculate MUCAPE. The highest CAPE medians were found it in the category 4 (745 J/kg for MUCAPE, 485 J/kg for SBCAPE and 65 MLCAPE). These events are characterized by a temperature near dew point in all layers and the parcels can rise from surface and there is not much further latent cooling of evaporation since air is already or nearly saturated.

It is interesting to note that in >75% of the cases, the MLCAPE, MUCAPE and SBCAPE values are below 1000 J/kg. In typical severe storm environments, CAPE values <1000 J/kg are usually considered small (Markowski and Richardson, 2010). These results are in agreement with those obtained by Sherburn and Parker (2014), who defined low CAPE environments by surface-based CAPE ≤500 J/kg and most unstable parcel CAPE ≤1000 J/kg. The values obtained in this research are also similar to those measured in the north-west of the Iberian Peninsula during hailfall episodes (López et al., 2001). However, these results differ from those obtained by Craven and Brooks (2004), with similar CAPE values in severe storms with and without hail. CAPE values calculated in Canary Islands are lower than the ones obtained during severe thunderstorms in China (Li et al., 2018), United States (Brooks et al., 2003) and even in Europe (Brooks et al., 2007; Tuovinen et al., 2015). The lower CAPE values characteristic of Canary Islands might be connected to the dry air commonly located above the trade-wind inversion layer. This fact highlights the need to adapt the convection index thresholds to the region of interest.

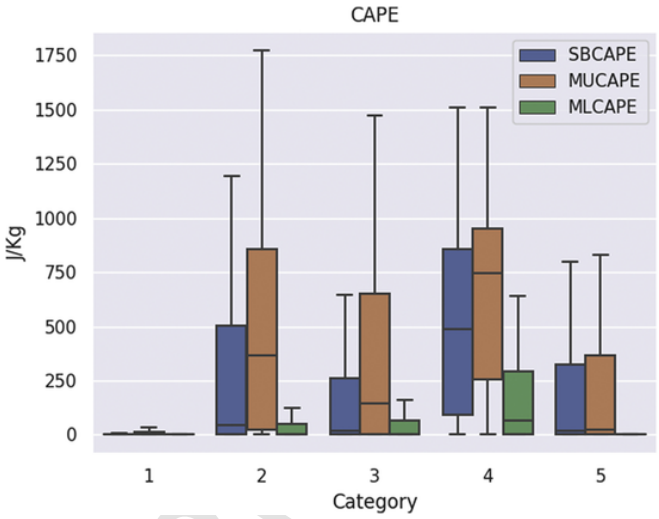

Fig. 2. Box and whisker plot of the lowest 100 hPa mean layer CAPE (J/kg), Most Unstable parcel found in the lowest 300 hPa CAPE (J/kg) and Surface Based parcel CAPE (J/kg).

4.1.2. Lapse rates

Low level (0–3 km and 850-700 hPa, Fig. 3 and Fig. 4) Environmental Lapse Rate (ELR) shows significant difference between category 1 and the rest of the categories. Category 1 shows 75% lapse rate values less than 5°C/Km, stable or absolutely stable. Conditionally unstable conditions predominate for the rest of the categories. Categories 4 and 5 show more than 75 percent of conditionally unstable conditions. This is consistent with the research carried out by Taszarek et al. (2017), in which higher lapse rates at low levels were found during hail and severe wind gust events. Our results are also in agreement with the conclusions of Jin et al. (2017), who detected that the midlevel temperature lapse rate was strongly correlated to hailfall in South Korea.

Analysing the upper layers of the atmosphere (3-6 km and 700-500hPa, Fig. 3 and Fig. 4), it is observed that instability increases with height for all categories except for category 4 where the me-

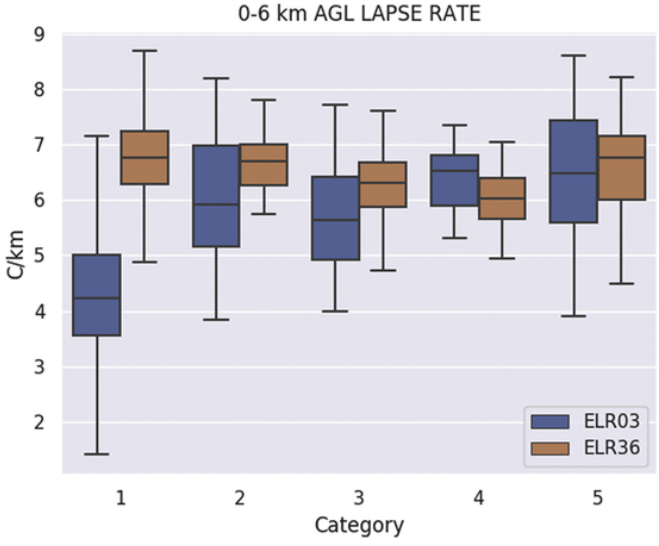

Fig. 3. Box and whisker plot of 0-3 km AGL Environmental Lapse Rate (°C/km) and 3-6 km AGL Environmental Lapse Rate (°C/km).

[1] We want to place the cite Fernández-González et al., 2016 in section 4.1.1 CAPE, after "strong winds are the most common severe weather.

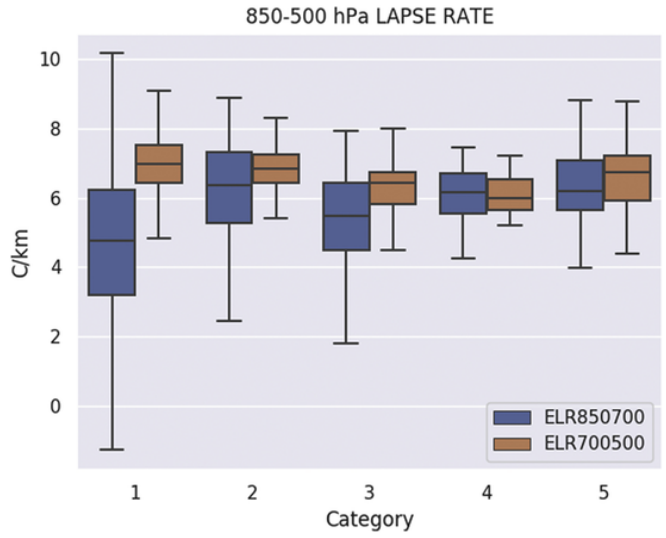

Fig. 4. Box and whisker plot of 850-700 hPa Environmental Lapse Rate (°C/km) and 700-500 hPa Environmental Lapse Rate (°C/km).

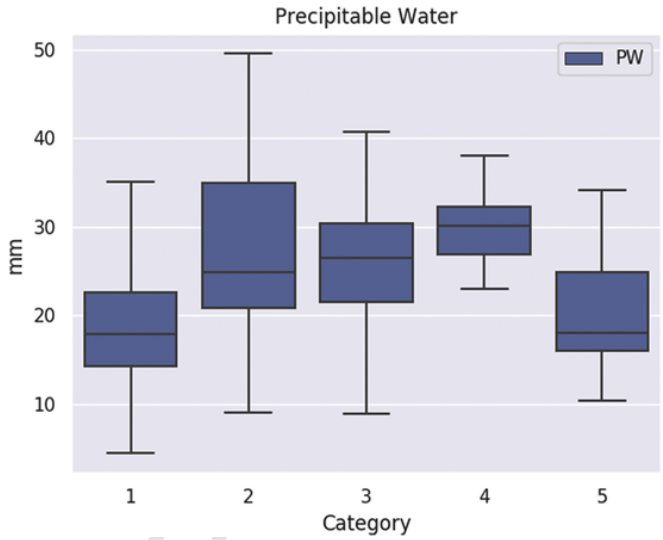

Fig. 5. Box and whisker plot of total precipitable water (mm).

dian goes from being 6.5°C/km (0-3 km AGL Lapse Rate) to 6°C/km (3-6 km AGL Lapse Rate). The results calculated for Canary Islands are consistent with those obtained by Craven and Brooks (2004) in the United States, although the no thunder category is more clearly discriminated in this research by the lapse rates between 0-3 km.

The explanation of the change in conditions from stable or absolutely stable to conditionally unstable with height in category 1, is due to the vertical structure of the atmosphere in the region under normal conditions. Trade winds, which blow towards Ecuador, come from higher latitudes and, as a result, act like cold masses. Above these winds, there is layer of the hottest and driest air in the world, so that the inversion that separates both air masses is extremely sharp and stable. However, that inversion has potential instability (also called convective instability or thermal instability), and just a column lift to subvert it. The negative lapse rates between 850-700 hPa in category 1 are related to the presence of a subsidence inversion.

According to Houston and Niyogi (2007), lapse rates are crucial in the development of convective clouds. They are connected to potential instability, which is the state of an unsaturated layer or column of air in the atmosphere with a wet-bulb potential temperature (or equivalent potential temperature) that decreases with elevation. If such a column is lifted bodily until completely saturated, it will become unstable (i.e., its temperature lapse rate will exceed the saturation-adiabatic lapse rate) regardless of its initial stratification (Saucier, 1955).

4.1.3. Total precipitable water

Total precipitable water (TPW) shows median values around 18 mm for categories 1 and 5 (Fig. 5). On the other hand, categories 2 and 3 with 75 percent exceed 20 mm while category 4 exceeds that threshold in 100 percent of the cases, placing its median around 30 mm.

Therefore, high TPW values (above 20 mm) are necessary for the occurrence of heavy rain events on the Canary Islands. Nevertheless, hailstorms can take place with TPW values below 20 mm, so it does not seem a transcendental factor in the hail development in the study area. These TPW values are slightly lower than those obtained by Li et al. (2018) during hailstorm events in China. In that research, the authors found a direct relationship between the TPW amount and the hail size. Similarly to CAPE, the reason of the TPW values in Canary Islands may be linked to the cold oceanic current that exists in the western shore of North Africa, as well as the dry air above the trade-wind inversion.

4.1.4. LCL height

The median values of LCL height (Fig. 6) in the categories 1, 2 and 5 are around 1000 m AGL. Categories 3 and 4 (all related to heavy rainfall) show medians around 830 meters. Since moisture in the planetary boundary layer is related to the LCL (Li et al., 2018), these results indicate that high moisture in the boundary layer is necessary for the occurrence of heavy rain events, while it is not indispensable for the development of thunderstorms or hailstorms. Our results are in agreement with those of Taszarek et al. (2017), who claimed that large hailstorm and severe wind gusts events take place with higher cloud bases than the non-severe thunderstorm events. Since relatively low moisture in the boundary layer is related to more low-level cooling through sublimation, melting and evaporation of falling precipitation, stronger outflow are generated, increasing the likelihood of severe wind gusts (Rasmussen and Blanchard, 1998).

4.1.5. Vertical wind shear

In general, wind shear increases with height for all categories (Fig. 7).The most relevant feature is that the median values of categories 3, 4 and 5 are around 40 kt for 0-6 km layer (Fig. 7) and the category 1 can be discriminated because in more than 75 percent of the cases 0-

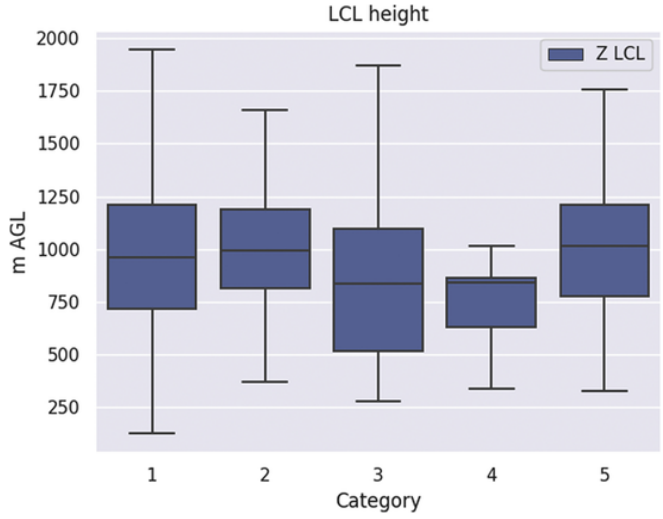

Fig. 6. Box and whisker plot of LCL height (m AGL).

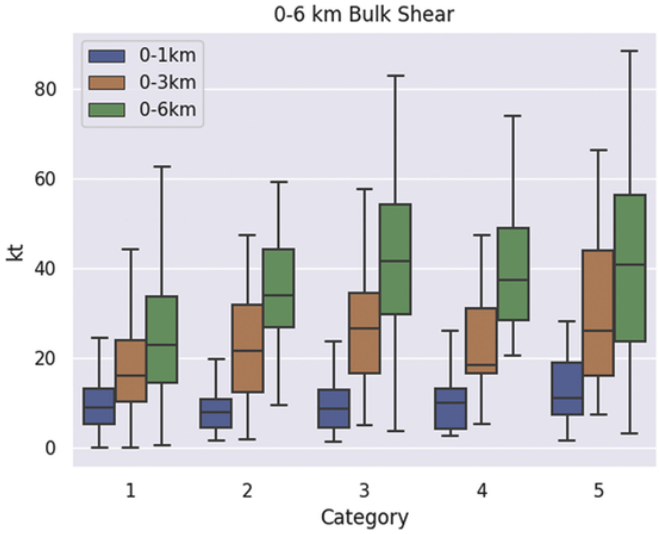

Fig. 7. Box and whisker plot of 0-1 km shear, 0-3 km shear and 0-6 km shear (kt).

6 km Bulk shear do not reach the 40 kt threshold. Category 5 shows the highest median of low level wind shear, (0-1 km Bulk shear, Fig. 7) around 12 kt. In fact, hail or wind gust ≥ 120 km/h events are characterized by high 0–6 km bulk shear vector magnitude (Fig. 7) and Low CAPE. Our results agree with those obtained by Sherburn and Parker (2014), who linked High-Shear environments of 0–6 km shear vector magnitude ≥ 35 kt with hail events. In addition, Taszarek et al. (2017) asserted that the risk of hailstorms increase along with higher values of wind shear, being this the best parameter for assessing the severity of deep convection events. Our results are also consistent with those obtained by Jin et al. (2017), who detected a strong correlation between strong bulk wind shear and hail occurrence.

Severe weather episodes were recorded with a broad range of CAPE and shear values (Schneider and Dean, 2008). Therefore, the high dispersion observed in the box and whisper plots of bulk shear for category 5 may be related to the wide variety of meteorological conditions that can trigger strong winds during convective events (Taszarek et al., 2017). Severe convective storms in environments with large vertical wind shear but meagre instability [high-shear, low-CAPE (HSLC) environments] have received only modest attention in the literature compared to their higher-CAPE counterparts (Sherburn and Parker, 2014). However, Craven and Brooks (2004) related High-Shear environments with risk of significant tornadoes.

4.1.6. Other parameters computed

In addition to the parameters calculated in the previous subsections, other parameters were computed. In the case of storm relative helicity (0-1 km and 0-3 km, graphs not shown), no relevant conclusions were found. Nevertheless, remarkable results were obtained in the case of thicknesses analysis. Several thicknesses were calculated: 1000-850 hPa, 1000-700 hPa, 1000-500 hPa, 850-700 hPa (graphs not shown). All thicknesses computed show notable differences. The medians values for category 5 is considerably smaller than other categories. Empirical studies (e.g., Glahn and Bocchieri, 1975; Cantin and Bachand, 1993) have shown that certain values of differing thickness have shown some skill in differentiating between rain and snow.

Table 3.
Critical thickness in meters.

Thickness	Critical thickness values (meters)
1000-850 hPa	1365
1000-700 hPa	2936
1000-500 hPa	5550
850-700 hPa	1572

In this way, empirical thresholds based on medians values of different thickness (from category 5 events) have been established in the Canary region as critical thickness, to distinguish between the precipitation types. Table 3 shows the critical thickness values for different atmospherics layers on the Canary Islands. These values can be used to help the precipitation type forecasting in this area. In applying these values to forecast, if thickness values are less than the critical thickness value, snow is the likely precipitation type. If thickness values are greater than the critical thickness value, rain is the likely precipitation type. Thickness values just provide a clue to the precipitation type, not the occurrence of the precipitation.

4.2. Seasonal and annual variability

The global distribution of seasonal and inter annual variations of CAPE and TPW during 2009–2018 are analyzed in this section. First, the left panel of Fig. 8 displays the monthly average values of CAPE. Medians values around 0 J/kg are obtained for much of the year, except in autumn (September, October, November), when the median increases to around 50 J/Kg. The seasonal cycle of CAPE is defined by the seasonal cycles of temperature and specific humidity. Higher values are generally found in the autumn for the Canary Islands. In contrast to the global distribution of seasonally averaged CAPE (Riemann-Campe et al., 2009), where higher values are generally found in the summer northern hemisphere (June, July, and August, JJA). These differences are due to the strength of the subsidence inversion in summer (JJA) in the Canary Islands. The inversion suppresses convection by acting as a cap. Therefore, an air parcel rising into the inversion layer would sink back to its original level because the rising parcel would be colder and denser than the air surrounding it.

Inter annual variations of CAPE (right panel of Fig. 8) show small median differences between years. However, the 75th percentile presents notable differences between years, mainly the years 2014, 2015 and 2017 where it reaches 200 J/kg. Data grouped by season (Fig. 9) highlights the winter (DJF) of 2010 and the spring (MAM) of 2017. The high values of CAPE in the winter of 2010 are in agreement with

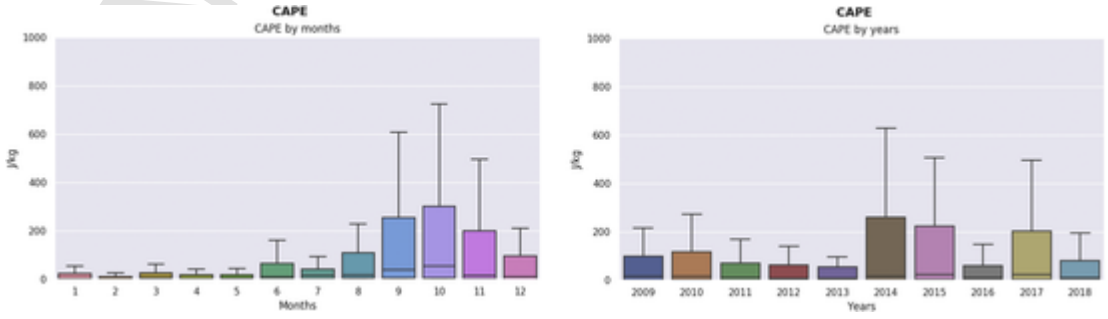

Fig. 8. Box and whisker plot of CAPE (J/kg) group by months (left) and by years (right).

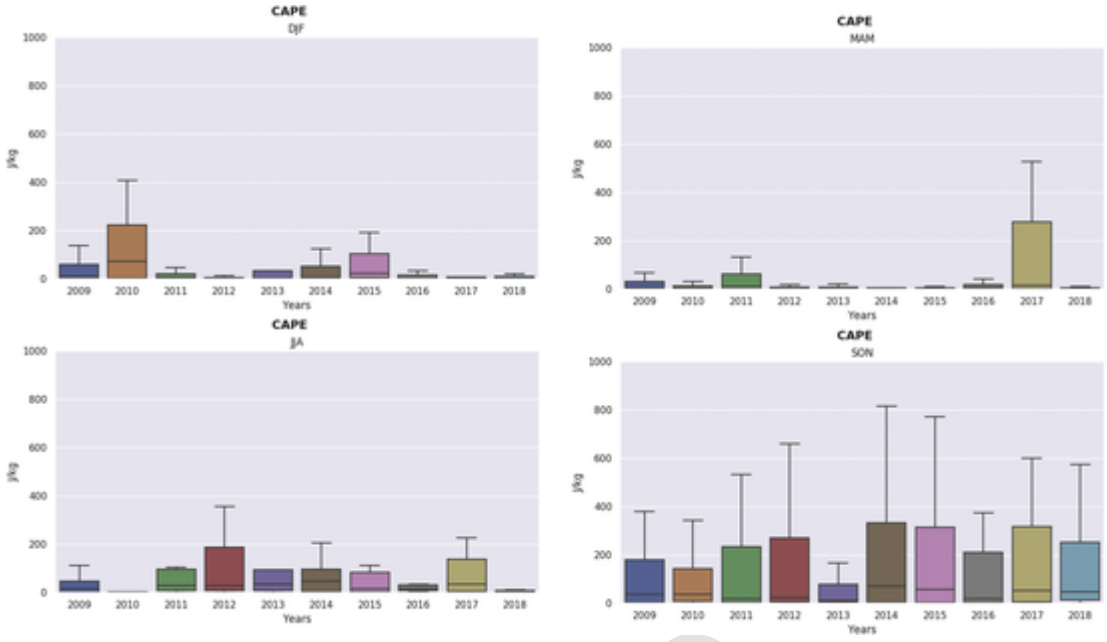

Fig. 9. Box and whisker plot of CAPE (J/kg) group by season.

the results obtained by Núñez Mora et al. (2019), who indicated that this year was the one with the highest number of storm days in the Canary Islands, with 80 days (studied period 2007-2016).

Seasonal cycle of TPW is quite similar to CAPE's cycle. TPW median values are between 10 to 20 mm throughout the year (left panel of Fig. 10) but these values rise above that 20 mm threshold during August, September and October, and then decrease again in November. These results are in agreement with those of Romero Campos et al. (2011), who claimed that, during these months, the air in contact with the sea surface is heated and has more capacity to store water vapour. Then, the updrafts and downdrafts associated to convection spread water vapour more evenly throughout the entire column. The right panel of Fig. 10 shows inter annual variations of TPW. Note that the annual median is close to 20 mm and that there are no marked differences between years, being inter annual variability of TPW much lower than that of CAPE. As shown in Fig. 11, the TPW was also remarkably high during the winter of 2010.

4.3. Case studies

In this section, the parameters derived from the radio soundings are analysed in detail for two case studies. Both situations correspond to events before 2009 and therefore not included in the statistics calculated in the previous subsection. Case a) corresponds to a category 4 event, while case b) matches to a category 5 episode.

4.3.1. Case a (10/29/2006)

The synoptic situation was characterized by a blocking high (Fig. 12) on the north of the Iberian Peninsula extending to northern Europe, while the Canary Islands were affected by a low pressure system with a minimum sea level pressure of 1012 hPa. At 500 hPa, the low system was located on the north of the Canary Islands with a core temperature around -18 °C. The heaviest rainfall in one hour (Fig. 13) occurred in the south of La Gomera (53.5 mm in an hour).

4.3.2. Case b (02/19/2004)

In case b), the Canary Islands were affected by an intense extra-tropical cyclone (with a minimum of sea level pressure of 994 hPa, Fig. 14), causing strong west-southwest wind over the region. In 500 hPa the low system was located northwest of the islands with a core temperature around -24 °C. The heaviest rainfall accumulated in one hour during this event is shown in Fig. 15. El Hierro was the most affected island (15.2 mm in an hour), being the rainfall accumulated in one hour considerably lower than that registered during episode a). Nevertheless, wind gusts were more intense in this event (Fig. 16). Although the threshold of 120 km/h was not reached, hail was observed in at least 2 locations and, as a result, this event belongs to category 5.

Table 4 shows the values of the calculated parameters for both situations. The results of case studies are of great interest because they are consistent with the results obtained for categories 4 and 5 in the previous section. Therefore, the characterization and knowledge of

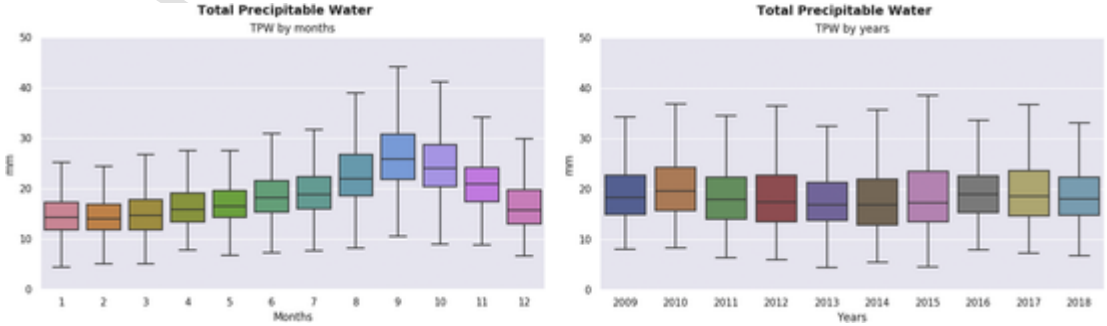

Fig. 10. Box and whisker plot of Total Precipitable Water (mm) group by months (left) and by years (right).

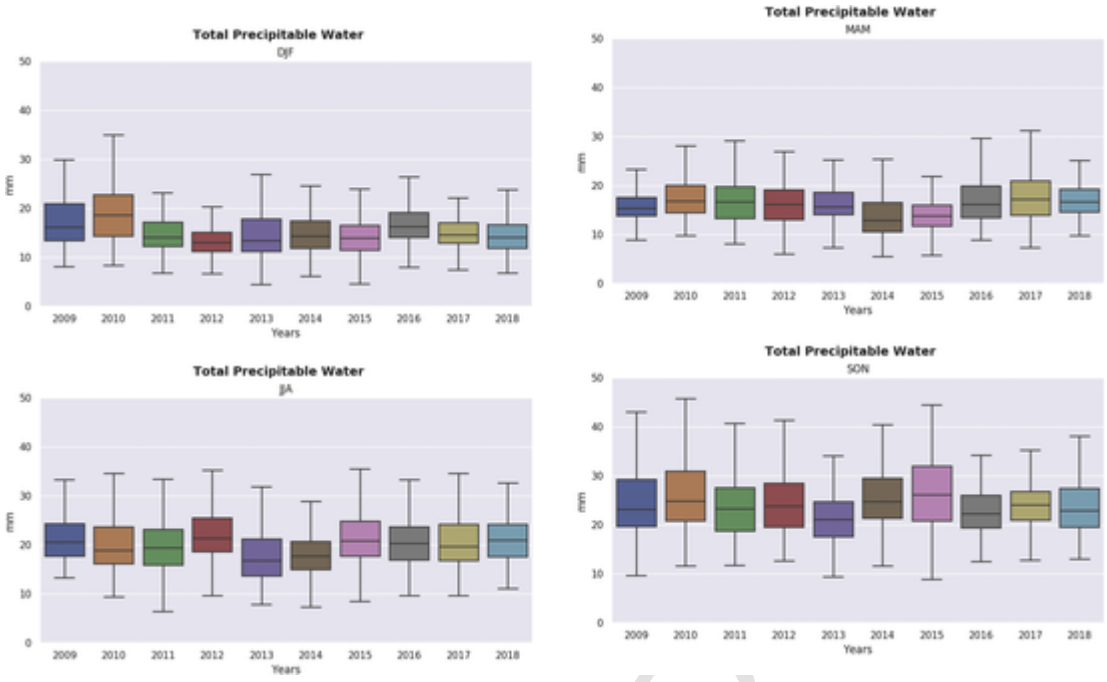

Fig. 11. Box and whisker plot of Total Precipitable Water (mm) group by season.

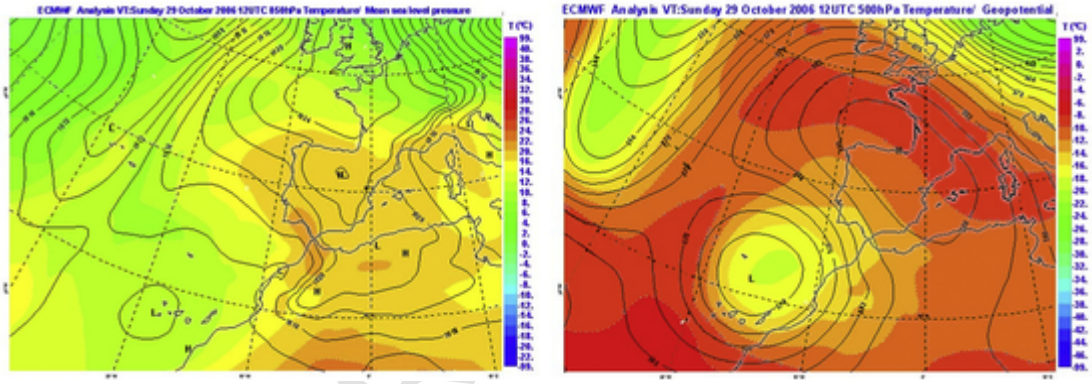

Fig. 12. Analysis from ECMWF model (29 October 2006 12 UTC). Left: Mean sea level pressure and 850 hPa temperature. Right: 500 hPa temperature and geopotential (Source: AEMET).

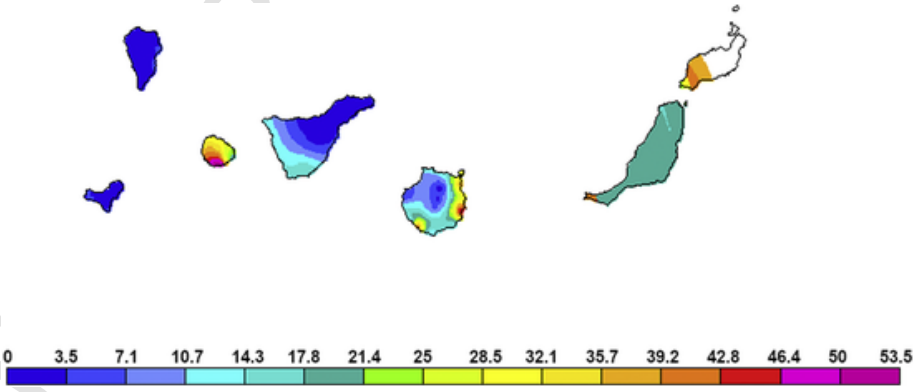

Fig. 13. Maximum 1 hour rainfall (mm) in 29 October of 2006 (Source: AEMET).

the different indices used in this article for the Canary Islands is relevant for operational use.

As illustrated by case a), extreme precipitation events (category 4, rainfall ≥ 30 mm /h) in the Canary Islands are characterized by high values of MUCAPE and SBCAPE compared to those obtained in the other categories in the region of interest. In addition, in these situations the lapse rate decreased with height, moving from a conditionally unstable layer (0-3 km) to a stable layer (3-6 km), and high content of TPW are presented. When a capping inversion is present but weak, or non-existent, convection can readily break out. However, in cases

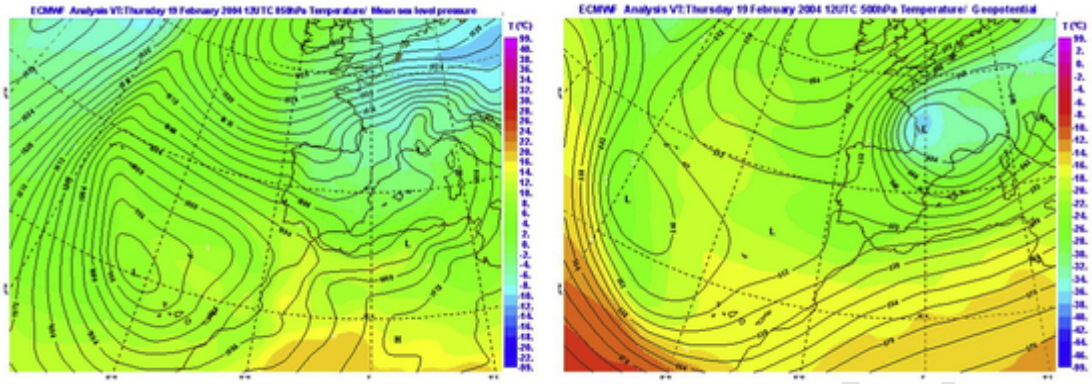

Fig. 14. Analysis from ECMWF model (19 February 2004 12 UTC). Left: Mean sea level pressure and 850 hPa temperature. Right 500 hPa temperature and geopotential (Source: AEMET).

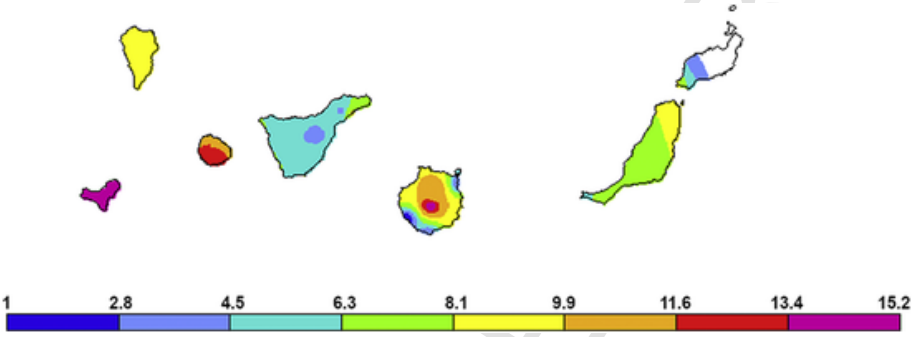

Fig. 15. Maximum 1 hour rainfall (mm) in 19 February of 2004 (Source: AEMET).

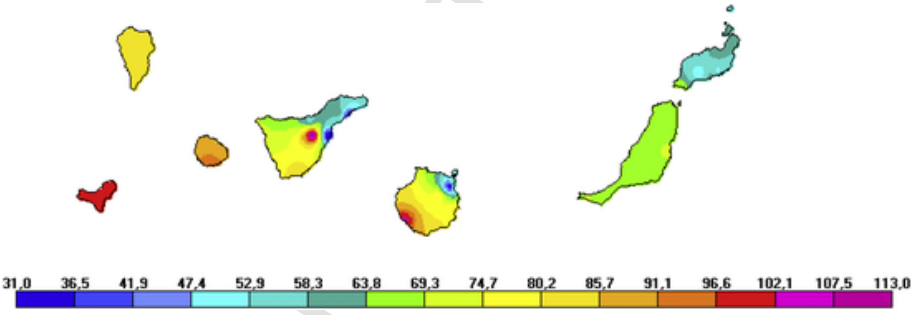

Fig. 16. Daily maximum wind gust (km/h) in 19 February of 2004 (Source: AEMET).

Table 4.
Parameters computed for both case studies.

Parameter	Case a	Case b	Units
MUCAPE	550	30	J/kg
MLCAPE	54	4	J/kg
SBCAPE	438	16	J/kg
0-3 km AGL Lapse Rate	6.1	5.7	°C/km
3-6 km AGL Lapse Rate	5.7	6.7	°C/km
LCL height (lifted condensation level)	392	932	m AGL
0-1 km Bulk shear	8.9	4.9	Kt
0-3 km Bulk shear	12.6	25.6	Kt
0-6 km Bulk shear	34.2	48.8	Kt
Total precipitable water	30	19	mm

of stronger capping inversions, dry surfaces may be more conducive to deep convection even if there is less moisture since the larger sensible heat flux in those cases can erode the capping layer (McGinley, 1986). In these events, the precipitation intensity is related to the amount of water vapour that is condensed in a convective updraft and the speed with which the condensation occurs. Hence, both strong instability that leads to strong updrafts and a high amount of water vapour available for condensation are important for the precipitation rate. Convection that is sustained from a deep, moist boundary layer will likely produce storms with heavy precipitation.

On the other hand, the events framed in category 5 (hail or wind gust ≥ 120 km/h), according to case study b) and the results obtained in previous section, are characterized by a high 0–6 km bulk shear vector magnitude and Low CAPE (HSLC). HSLC environments were previously defined by 0–6 km shear vector magnitude ≥ 35 kt, surface-based CAPE ≤ 500 J/kg and most unstable parcel CAPE ≤ 1000 J/kg. In addition, in these situations the lapse rate increased with height and low content of TPW are presented. These events have dry air in the lower troposphere with nearly saturated air in the middle troposphere and the convection tends to be high based.

In events of category 5, wind shear has an important influence on deep convection because it plays a role in the generation of new convective cells along the outflow of an older cell and hence influences the propagation of a storm system and it affects vertical speeds in

storm updrafts and downdrafts, by causing pressure perturbations. Deep layer shear strongly influences convective organization.

4.4. Simulated soundings application

The operational forecast of convective episodes is more difficult in subtropical regions such as the Canary Islands since the performance of numerical weather prediction models is lower than in the extra-tropics (Žagar et al., 2005). The categorization carried out in this research can provide a quantification of the risk of occurrence of a certain meteorological phenomenon when the thresholds defined in the previous section are exceeded. In order to apply this technique to operational forecasting, we need to anticipate the information provided by the observed radio sounding. That is why this section presents the possibility of using forecast soundings obtained from numerical models. The soundings from high resolution models are used extensively in severe weather forecasting. Nowadays, the increase in the resolution of the numerical models makes them closer to the observation. In this regard, simulated soundings from Integrated Forecasting System (IFS) of the ECMWF for both study cases and observed sounding are shown (Fig. 17 and Fig. 18). For case study a) (Fig. 17), both soundings showed similar values of Total Precipitable Water and shear. However, CAPE's values were underestimated by simulated sounding. Due to the vertical (in 2006 operational ECMWF model had 91 levels) and horizontal resolutions the main differences have been found in low levels because the nearest grid model point is at a higher altitude than observation.

For case study b) (Fig. 18), despite the worst vertical resolution (in 2004 operational ECMWF model had only 60 levels) both soundings were quite similar. The low and middle levels show again the most remarkable differences. While observed sounding presents up to four temperature inversions in the low and middle levels, the simulated sounding shows only one. This is obviously due to the vertical discretization of the model.

In the first stage of convective forecasting, the operational forecaster needs data about the current weather situation to make a diagnosis. As shown above, the atmospheric conditions can be acceptably reproduced by the soundings forecasted by the IFS model. The incessant improvements in the resolution of the models make them reproduce the atmospheric conditions more precisely. In this regard, the high resolution forecast of the IFS model currently has a horizontal resolution of 9 km, and 137 vertical levels. In addition, the HARMONIE-AROME is the operative mesoscale model used in AEMET, which has a horizontal resolution of 2.5 km and 65 vertical levels. Simulated soundings provided by the HARMONIE-AROME and IFS can be really useful for making a reasonable analysis, and it can be used as a tool to predict the evolution of the weather in the short-term.

Although the performance of numerical models about the development of convective storms in subtropical regions is not very accu-

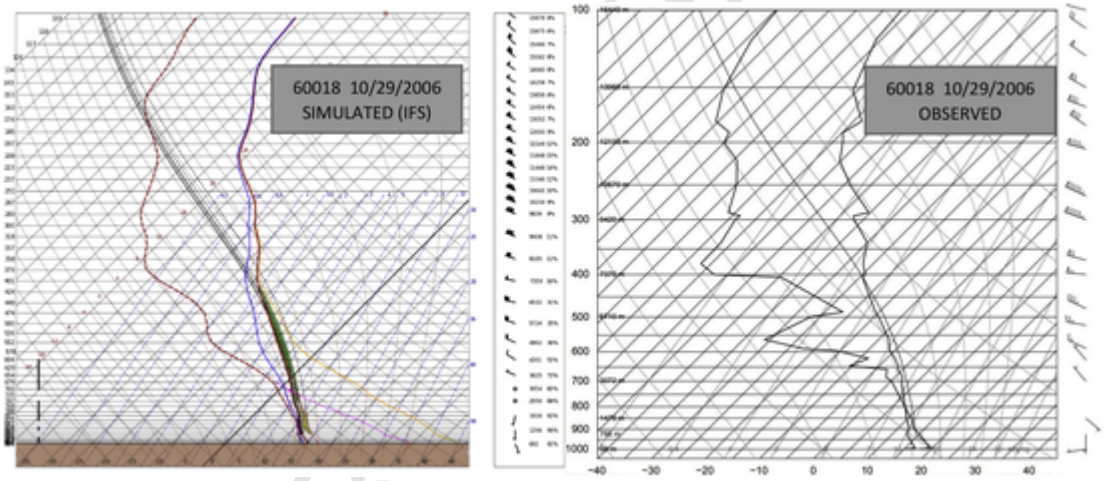

Fig. 17. Simulated and observed soundings for the case study a) (10/29/2006). Sounding forecasted by the IFS model (left panel) on the nearest grid model point to 60018 radio sounding station (Source: AEMET). Right panel shows the observed sounding from 60018 station (Source: University of Wyoming).

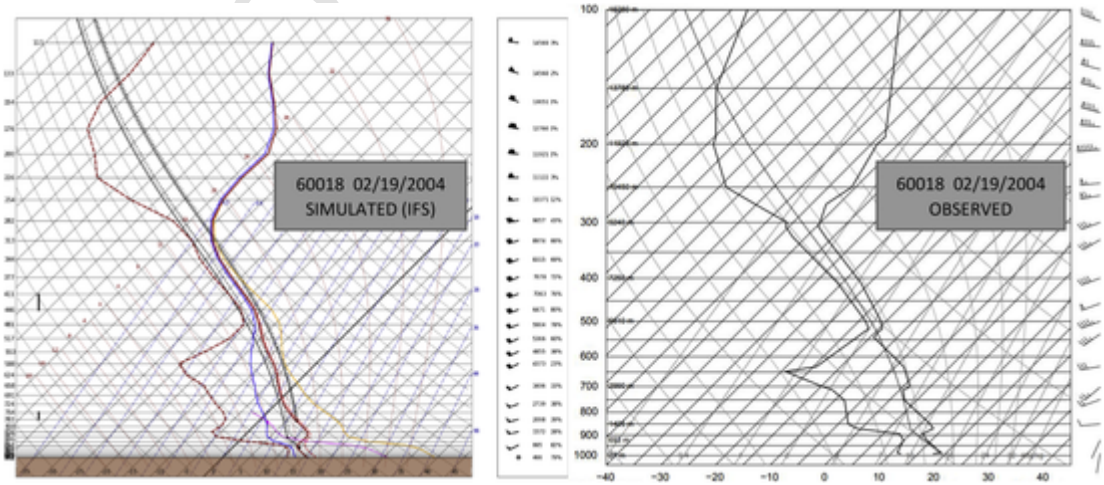

Fig. 18. Simulated and observed soundings for the case study b (02/19/2004). Sounding forecasted by the IFS model (left panel) on the nearest grid model point to 60018 radio sounding station (Source: AEMET). Right panel shows the observed sounding from 60018 station (Source: University of Wyoming).

rate, the use of convective indices obtained from forecast soundings can be useful in the diagnosis of the situation. The classification within the 5 categories defined in this research can be useful in the decision-making process when the operational forecaster has to evaluate the risk of a certain weather phenomena.

5. Conclusions

In this research, different indices from soundings were computed from the analysis of 7021 soundings from the Güimar station (id = 60018, Tenerife) during the period 2009-2018. Subsequently, a classification of the values of these indices was made according to the observed meteorological phenomena. The results can be summarised by the following remarkable conclusions:

- CAPE values were below 1000 J/kg in more than 75 percent of the cases on the Canary Islands.
- In the area of interest, extreme rainfall events (rainfall > 30 mm/h) are characterized by the highest median of MUCAPE and SBCAPE, a decrease of Environmental Lapse Rate with height, and high TPW. However, categories 2 and 3 showed SBCAPE median values close to 0. In addition, the analysis of CAPE values can be used to discriminate category 1 (no thunder) from the rest.
- In the Canary Islands, hail or wind gusts higher than 120 km/h events are characterized by high 0–6-km bulk Shear vector magnitude (HS) and Low CAPE (LC), besides low TPW.
- Seasonal cycle of CAPE in the Canary Islands showed differences with global distribution of CAPE. These differences are due to the strength of the subsidence inversion in summer in the Canary Islands, which acts as a lid inhibiting convection.
- The largest median values of TPW are found during August, September and October, when the highest sea surface temperatures are reached in the Canary Islands and, consequently, the air in contact with the sea surface has more capacity to store water vapour.
- In this study, it has become evident that the combination of sounding derived parameters can help the operational forecaster to evaluate the risk of adverse weather phenomenon. In order to illustrate the application of the combined use of different parameters, 2 case studies were analysed. Both cases showed similar behaviour to the results obtained with the complete data set, supporting the importance of the characterization and knowledge of environmental conditions for severe thunderstorms in the region of interest.
- Sounding data analysis can be useful to understand what kinds of atmospheric conditions are typically observed during severe thunderstorm event. They help aid forecasters in knowing when unusual conditions are occurring. In weather forecasting, it is extremely important for forecaster to recognize unusual conditions when they come together. Local studies of the frequency of occurrence of unusual conditions can be a great aid.
- In this study, forecast soundings from high resolution models showed good ability to reproduce the observed conditions. Therefore, the use of forecast soundings is recommended in order to anticipate the risk of a severe weather event.

The conclusions of this paper could significantly aid the operational forecasters of AEMET in the Canary Islands during the decision-making process of warning the population and Civil Protection Authorities about the occurrence of severe weather events, raising alerts regarding thunderstorms, heavy rain, gale-force winds and hail risk.

Author statement

The paper entitled "Analysis of sounding derived parameters and application to severe weather events in the Canary Islands" was carried out by the authors David Suárez Molina, Sergio Fernández-González, Juan Carlos Suárez González and Albert Oliver. In the following lines, the contribution of each author will be detailed:

David Suárez Molina: He is the main contributor to this paper, being the responsible of the conceptualization, design of the methodology, obtaining results, and writing.

Sergio Fernández-González has contributed in the redaction of the paper, and supervising the research activity.

Juan Carlos Suárez González has helped with the software, data curation and formal analysis.

Albert Oliver has contributed in the second revision and the analysis of the radio soundings incorporated in this version of the manuscript.

Uncited references

Fernández-González et al., 2016

Declaration of Competing Interest

The authors claim that there is no conflict of interest, nor any funding source that intercedes with the free publication of results obtained in this research.

Acknowledgments

Data support came from the State Meteorological Agency of Spain (AEMET). The observed soundings were supplied by University of Wyoming (http://www.weather.uwyo.edu/upperair/sounding.html). Special thanks go to the SAFEFLIGHT (CGL2016-78702-C2-1-R and CGL2016-78702-C2-2-R) and UE ERA-NET Plus NEWA (PCIN2016-080) projects.

References

Bauer, P., Thorpe, A., Brunet, G., 2015. The quiet revolution of numerical weather prediction. Nature 525, 47–55. doi:10.1038/nature14956.

Bolgiani, P., Fernández-González, S., Valero, F., Merino, A., García-Ortega, E., Sánchez, J.L., Martín, M.L., 2018. Numerical Simulation of a heavy precipitation event in the vicinity of Madrid-Barajas international airport: sensitivity to Initial conditions, domain resolution, and microphysics parameterizations. Atmosphere 9, 329. doi:10.3390/atmos9090329.

Borsky, S., Unterberger, B.C., 2019. Weather and flight delays: The impact of sudden and slow onset weather events. Econ. Transp. 18, 10–26.

Brooks, H.E., Doswell, C.A., III, Cooper, J., 1994. On the environments of tornadic and nontornadic mesocyclones. Wea. Forecasting 9, 606–618.

Brooks, H.E., Lee, J.W., Graven, J.P., 2003. The spatial distribution of severe thunderstorm and tornado environments from global reanalysis data. Atmos. Res. 67–68, 73–94.

Brooks, H.E., Anderson, A.R., Riemann, K., Ebbers, I., Flachs, H., 2007. Climatological aspects of convective parameters from the NCAR/NCEP reanalysis. Atmos. Res. 83, 294–305. doi:10.1016/j.atmosres.2005.08.005.

Cantin, A., Bachand, D., 1993. Synoptic pattern recognition and partial thickness techniques as a tool for precipitation types forecasting associated with a winter storm. Centre Meteorologique du Quebec Tech. Note 93N-002, 9 pp. [Available from Environmental Weather Services Office, 100, boul. Alexis-Nihon, Suite 300, Saint-Laurent, PQ H4M 2N8, Canada].

Charba, J.P., 1979. Two-to-six hour severe local storm probabilities: An operational forecasting system. Mon. Weather Rev. 107, 268–282.

Craven, J.P., Brooks, H., 2004. Baseline climatology of sounding derived parameters associated with deep, moist convection. Natl. Wea. Dig. 28, 13–24.

Craven, J.P., Jewell, R.E., Harold, H.E., 2002. Comparison between Observed Convective Cloud-Base Heights and Lifting Condensation Level for Two Different Lifted Parcels. Weather Forecast. 17, 885–890. doi:10.1175/1520-0434(2002)017<0885:CBOCCB>2.0.CO;2.

Czernecki, B., Taszarek, M., Kolendowicz, L., Konarski, J., 2016. Relationship between human observations of thunderstorms and the PERUN lightning detection network in Poland. Atmos. Res. 167, 118–128. doi:10.1016/j.atmosres.2015.08.003.

Darkow, G.L., 1969. An analysis of over sixty tornado proximity soundings. Preprints. In: 6th Conf. on Severe Local Storms, Chicago, IL, Amer. Meteor. Soc, pp. 218–221.

Dorta, P., 2007. Catálogo de riesgos climáticos en Canarias: Amenazas y vulnerabilidad. Geographicalia, ISSN 0210-8380, N° 51, 2007 133-160. 51. doi:10.26754/ojs_geoph/geoph.2007511118.

Doswell, C., III, 1987. The Distinction between Large-Scale and Mesoscale Contribution to Severe Convection: A Case Study Example. Weather Forecast. 2, 3–16. doi:10.1175/1520-0434(1987)002<0003:TDBLSA>2.0.CO;2.

Doswell, C., III, Rasmussen, E., 1994. The Effect of neglecting the virtual temperature correction on CAPE calculations. Weather Forecast. 9, 625–629. doi:10.1175/1520-0434(1994)009<0625:TEONTV>2.0.CO;2.

Fernández-González, S., Wang, P.K., Gascón, E., Valero, F., Sánchez, J.L., 2016. Latent cooling and microphysics effects in deep convection. Atmos. Res. 180, 189–199. doi:10.1016/j.atmosres.2016.05.022.

Font, I., 1956. El Tiempo Atmosférico en las Islas Canarias. Servicio Meteorológico Nacional 96.
García-Ortega, E., Hermida, L., Hierro, R., Merino, A., Gascón, E., Fernández-González, S., Sánchez, J.L., López, L., 2014. Anomalies, trends and variability in atmospheric fields related to hailstorms in north-eastern Spain. Int. J. Climatol. 34, 3251–3263. doi:10.1002/joc.3910.
García-Ortega, E., Lorenzana, J., Merino, A., Fernández-González, S., López, L., Sánchez, J.L., 2017. Performance of multi-physics ensembles in convective precipitation events over northeastern Spain. Atmos. Res. 190, 55–67. doi:10.1016/j.atmosres.2017.02.009.
Gascón, E., Merino, A., Sánchez, J.L., Fernández-González, S., García-Ortega, E., López, L., Hermida, L., 2015. Spatial distribution of thermodynamic conditions of severe storms in southwestern Europe. Atmos. Res. 164–165, 194–209. doi:10.1016/j.atmosres.2015.05.012.
Génova, M., Máyer, P., Ballesteros-Cánovas, J.A., Rubiales, J.M., Saz, M.A., Díez-Herrero, A., 2015. Multidisciplinary study of flash floods in the Caldera de Taburiente National Park (Canary Islands, Spain). CATENA 131, 22–34. doi:10.3390/geosciences8080300.
Glahn, H.R., Bocchieri, J., 1975. Objective estimation of the conditional probability of frozen precipitation. Mon. Weather Rev. 103, 3–15. doi:10.1175/1520-0493(1975)103<0003:OEOTCP>2.0.CO;2.
Hamill, T.M., Church, A.T., 2000. Conditional probabilities of significant tornadoes from RUC-2 forecasts. Wea. Forecasting 15, 461–475.
Herrera, R.G., Puyol, D.G., Martín, E.H., Presa, L.G., Rodríguez, P.R., 2001. Influence of the North Atlantic Oscillation on the Canary Islands Precipitation. J. Climate 14, 3889–3903. doi:10.1175/1520-0442(2001)014<3889:IOTNAO>2.0.CO;2.
Houston, A.L., Niyogi, D., 2007. The sensitivity of convective initiation to the lapse rate of the active cloud-bearing layer. Mon. Weather Rev. 135, 3013–3032.
Jin, H.-G., Lee, H., Lkhamjav, J., Baik, J.-J., 2017. A hail climatology in South Korea. Atmos. Res. 188, 90–99. doi:10.1016/j.atmosres.2016.12.013.
Li, M.X., Sun, J.S., Zhang, Q.H., 2018. A Statistical Analysis of Hail Events and Their Environmental Conditions in China during 2008-15. J. Appl. Meteorol. Climatol. 57 (12), 2817–2833. doi:10.1175/JAMC-D-18-0109.1.
López, L., Marcos, J.L., Sánchez, J.L., Castro, A., Fraile, R., 2001. CAPE values and hailstorms on north western Spain. Atmos. Res. 56, 147–160.
López, L., García-Ortega, E., Sánchez, J.L., 2007. A short-term forecast model for hail. Atmos. Res. 83, 176–184. doi:10.1016/j.atmosres.2005.10.014.
Lorenc, A.C., Barker, D., Bell, R.S., Macpherson, B., Maycock, A.J., 1996. On the use of Radiosonde Humidity Observations in mid-latitude NWP. Meteorol. Atmos. Phys. 60, 3–17.
Markowski, P., Richardson, Y., 2010. Mesoscale Meteorology in Midlatitudes. doi:10.1002/9780470682104.
McGinley, J.A., 1986. Nowcasting mesoscale phenomena. In: Ray, P.S. (Ed.), Mesoscale Meteorology and Forecasting. In: Amer. Meteor. Soc.. pp. 657–688.
Merino, A., Sánchez, J.L., Fernández-González, S., García-Ortega, E., Marcos, J.L., Berthet, C., Dessens, J., 2019. Hailfalls in southwest Europe: EOF analysis for identifying synoptic pattern and their trends. Atmos. Res. 215, 42–56. doi:10.1016/j.atmosres.2018.08.006.
METEOALERTA, 2018. Plan Nacional de Predicción y Vigilancia de Fenómenos Meteorológicos Adversos. METEOALERTA. Agencia Estatal de Meteorología (AEMET). http://www.aemet.es/documentos/es/eltiempo/prediccion/avisos/plan_meteoalerta/plan_meteoalerta.pdf. (accessed 26 July 2019).
Meteorología, 2019. Ministerio para la Transición Ecológica. Madrid. NIPO: 014-18-005-8. (101 pp).
Núñez Mora, J.A., Riesco Martín, J., Mora García, M.A., 2019. Climatología de descargas eléctricas y días de tormenta en España. In: Agencia Estatal de Meteorología. Ministerio para la Transición Ecológica. Madrid. NIPO: 639-19-007-7.
Orville, R.E., 1991. Lightning ground flash density in the contiguous United States-1989. Mon. Weather Rev. 119, 573–577.
Púcik, T., Groenemeijer, P., Rýva, D., Kolár, M., 2015. Proximity soundings of severe and non-severe thunderstorms in central Europe. Mon. Weather Rev. 143, 4805–4821.
Rasmussen, E.N., Blanchard, D.O., 1998. A baseline climatology of sounding-derived supercell and tornado forecast parameters. Wea. Forecasting 13, 1148–1164.
Reap, R.M., 1986. Evaluation of cloud-to-ground lightning data from the western United States for the 1983-1984 summer seasons. J. Climate Appl. Meteor. 25, 785–799.
Riemann-Campe, K., Fraedrich, K., Lunkeit, F., 2009. Global climatology of Convective Available Potential Energy (CAPE) and Convective Inhibition (CIN) in ERA-40 reanalysis. Atmos. Res. 93, 534–545. doi:10.1016/j.atmosres.2008.09.037.
Romero Campos, P.M., Marrero de la Santa Cruz, C.L., Alonso Pérez, S., Cuevas Agulló, E., Afonso Gómez, S., Ortiz de Galisteo Marín, J.P., 2011. Una Climatología del Agua Precipitable en la Región Subtropical sobre la Isla de Tenerife basada en Datos de Radiosondeos. NT 6, Agencia Estatal de Meteorología. NIPO: 281-12-007-5.
Sánchez, J.L., López, L., Bustos, C., Marcos, J.L., García-Ortega, E., 2007. Short-term forecast of thunderstorms in Argentina. Atmos. Res. 88, 36–45.
Saucier, W.J., 1955. Principles of Meteorological Analysis. University of Chicago Press, p. 438. doi:10.1002/qj.49708235217.
Schaefer, J.T., Livingston, R.L., 1988. The structural characteristics of tornado proximity soundings. Preprints. In: 15th Conf. on Severe Local Storms, Baltimore, MD, Amer. Meteor. Soc, pp. 537–540.
Schneider, R.S., Dean, A.R., 2008. A comprehensive 5-year severe storm environment climatology for the continental United States. Preprints, 24th Conf. on Severe Local Storms, Savannah, GA, Amer. Meteor. Soc., 16A.4. [Available online at https://ams.confex.com/ams/pdfpapers/141748.pdf].
Sherburn, K.D., Parker, M.D., 2014. Climatology and Ingredients of Significant Severe Convection in High-Shear, Low-CAPE Environments. Wea. Forecasting 29, 854–877. doi:10.1175/WAF-D-13-00041.1.
Suárez-Molina, D., Fernández-Monistrol, J.A., Uriel-González, A.E., 2018. Catálogo-guía de fenómenos meteorológicos que afectan a la isla de Gran Canaria. Agencia Estatal de.
Taszarek, M., Brooks, H.E., Czernecki, B., 2017. Sounding-Derived Parameters Associated with Convective Hazards in Europe. Mon. Weather Rev. 145, 1511–1528.
Tukey, J.W., 1977. Exploratory Data Analysis. Addison Wesley 599.
Tuovinen, J.-P., Rauhala, J., Schultz, D.M., 2015. Significant-Hail-producing storms in Finland: convective-Storm environment and mode. Wea. Forecasting 30, 1064–1076. https://doi.org/10.1175/WAF-D-14-00159.1.
Wilks, D.S., 2011. Statistical Methods in the Atmospheric Sciences. 3rd ed. Academic Press, Oxford; Waltham, MA.
Žagar, N., Andersson, E., Fisher, M., 2005. Balanced tropical data assimilation based on study of equatorial waves in ECMWF short-range forecast errors. Q. J. R. Meteorol. Soc. 131, 987–1011.